Clinical Science (2020) **134** 1319–1331
https://doi.org/10.1042/CS20200249

PORTLAND PRESS

Research Article

TRIF/miR-34a mediates aldosterone-induced cardiac inflammation and remodeling

Shaojun Li[1,2], Wei Cao[1,2], Bai Wang[1,2], Enbo Zhan[1,2], Jian Xu[1,2] and Shufeng Li[1,2]

[1]Department of Cardiology, The Second Affiliated Hospital of Harbin Medical University, Harbin 150086, China; [2]The Key Laboratory of Myocardial Ischemia, Harbin Medical University, Ministry of Education, Heilongjiang Province, Harbin 150086, China

Correspondence: Shufeng Li (drlishufeng@163.com)

Aldosterone, as a major product of renin–angiotensin–aldosterone system (RAAS), determines multiple pathophysiological processes in cardiovascular diseases. The excess inflammatory response is one of the key profiles in aldosterone-mediated cardiac remodeling. However, the potential mechanisms of aldosterone/inflammatory signaling were still not fully disclosed. The present study aimed to investigate whether TIR-domain-containing adapter-inducing interferon-β (Trif) participated in the aldosterone-induced cardiac remodeling, and to explore potential molecular mechanisms. Trif knockout mice and their littermates were osmotically administrated with aldosterone (50 μg/kg per day) for 21 and 42 days. The cardiac structural analysis, functional parameters, and mitochondrial function were measured. Aldosterone dose- or time-dependently increased the levels of TRIF in primary mouse cardiomyocytes or mouse heart tissues. Trif deficiency protected against aldosterone-induced cardiac hypertrophy, fibrosis and dysfunction. Moreover, Trif deficiency also suppressed aldosterone-induced cardiac inflammatory response and mitochondrial injuries. Mechanistically, overexpression of cardiac microRNAs (miR)-34a reversed the cardiac benefits of Trif deficiency in aldosterone-treated mice. Taken together, Trif/miR-34a axis could provide a novel molecular mechanism for explaining aldosterone-induced cardiac hypertrophy, fibrosis and functional disorders.

Introduction

Cardiac pathophysiological remodeling is one of the major characteristics in the development of heart failure. There has been a sustained effort to develop novel strategies to protect against cardiomyopathy. Among them, agents that target the renin–angiotensin–aldosterone system (RAAS) are widely prescribed to combat heart failure [1]. Angiotensin-converting enzyme inhibitors, angiotensin receptor blockers, and mineralocorticoid receptor antagonists have significant therapeutic benefits in alleviating the morbidity and mortality of heart failure [2,3]. Although clinical trials and animal experiments have provided a variety of molecular findings, the underlying signaling pathways are still not fully understood. Therefore, it is necessary to disclose the mechanisms that RAAS affects cardiac structural and functional remodeling and the remaining challenges.

Aldosterone, as a prognostic and mediator of heart diseases, was significantly increased in patients from early cardiac injuries to more advanced heart failure [4]. Specific binding to the mineralocorticoid receptor (MR), aldosterone-activated multiple pathways to impair cardiac biological processes independently of blood pressure effects. Experimental findings showed that aldosterone-salt diet-induced rat cardiac fibrosis [5]. Aldosterone-salt-treated animals also exhibited progressive inflammatory phenotypes during cardiac hypertrophy [6,7]. In contrast, administration of spironolactone, a first-line of mineralocorticoid receptor antagonist, reduced the risk of mortality from any cause in patients with NYHA class III or IV heart failure [8]. Mechanistically, the inhibition of aldosterone/mineralocorticoid receptor binding activities blocked the downstream molecular signaling, including pro-inflammation, oxidative stress, and

Received: 02 March 2020
Revised: 15 May 2020
Accepted: 18 May 2020

Accepted Manuscript online: 19 May 2020
Version of Record published: 16 June 2020

Clinical Science (2020) **134** 1319–1331
https://doi.org/10.1042/CS20200249

calcium accumulation [9–11]. Among them, abnormal regulation of microRNAs (miRs) could determine the pathophysiological process of aldosterone in many tissues. MiRs, such as miR-21, miR-24 and miR-204, mediated tissue injuries and dysfunction in aldosterone-treated animals [12–14]. All these potential mechanisms supported the therapeutic benefits of pharmacological MR antagonism in treating heart failure.

Meanwhile, RAAS has been reported to activate Toll-like receptors (TLRs) as well as its downstream signaling cascade, such as myeloid differentiation primary response (MyD) 88 (MyD88) and TIR-domain-containing adapter-inducing interferon-β (Trif). In Ang II-infused mouse models, TLRs/MyD88/Trif pathways controlled the process of cardiac remodeling [15]. Trif deficiency attenuated Ang II-induced cardiac structural remodeling with down-regulation of cardiac expression of inflammatory genes [16]. According to multiple studies, activation of Trif stimulated inflammation and fibrosis in different tissues [17,18]. Due to the wide distribution in different organs and types of cells, Trif exhibited complicated physiological effects. However, it was unclear how Trif signaling affected RAAS-mediated cardiac remodeling. Therefore, it is necessary to specifically address the pathophysiological roles of cardiac Trif and potential molecular mechanisms in aldosterone-mediated cardiac biology.

To delineate the role of Trif in aldosterone-mediated cardiac remodeling, our present study utilized the genetic Trif knockout mouse model to disclose the potential molecular mechanisms. Our findings will link aldosterone and Trif signaling in cardiac remodeling, and provide evidence that therapeutic benefits of Trif inhibition in protecting against abnormal RAAS-induced heart failure.

Materials and methods

Reagents

The Hematoxylin and Eosin solution was purchased from Sigma chemicals (Sigma, St. Louis, U.S.A.). The Sirius Red (SR) stain kit was purchased from Abcam (#ab150681, Cambridge, U.K.). Anti-TRIF (#ab13810), anti-TGF-β1 (#ab92486), anti-phosphorylated (phos)-SMAD3 (#ab52903), anti-SMAD3 (#ab40854), anti-phos-IFN regulatory factor (IRF) 3 (IRF3) (#ab76493), IRF3 (#ab68481), and anti-Tubulin (#ab59680) antibodies were from Abcam (Cambridge, U.K.). Anti-atrial natriuretic peptide (ANP) and anti-brain natriuretic peptide (BNP) antibodies were from Novus (Novus Biologicals, CO). IFN-α antibody was purchased from Invitrogen (Thermo Fisher, MA). Measurement kit for cellular adenosine triphosphate (ATP) level was from Sigma chemicals (#213-579-1). Mouse kits for TNF-α (#MTA00B), IL-1β (#MLB00C), and nitric oxide (#KGE001) were from R&D (R&D Systems, MN). The adeno-associated viruses (AAVs) encoding miR-34 mimic and control with cardiac-specific α myosin-heavy chain (*Myh6*) promoter, and lentivirus encoding miR-34a sponge and control were a gift from Dr. Qian Ni (Tianjin University).

Primary cardiomyocyte isolation and treatment

Two to three days old neonatal mice were killed for isolating primary cardiomyocytes as previous procedure [19]. A total of 1×10^6 mouse primary cardiomyocytes were treated with different concentrations (0, 10^{-6}, 10^{-5}, 10^{-4} mol/l) of aldosterone for 24 h.

Animal experiment

All mouse experimental protocols were approved by the Institutional Animal Use and Care Committee at the Harbin Medical University (Harbin, China). Male Trif knockout mice and their littermates (the Jackson Laboratory), aged 8–10 weeks, were subcutaneously administrated with aldosterone (50 μg/kg per day, dissolved in saline) for 21 or 42 days by osmotic pumps. For mouse experiments of cardiac miR-34a overexpression, Trif knockout mice were tail-vein injected with 1×10^9 AAV encoding miR-34a mimic or control with cardiac-specific *Myh6* promoter for 14 days, then treated with aldosterone (50 μg/kg per day) by using osmotic pump for 21 days. Systolic arterial blood pressure was measured at 0, 7, 21 days after infusion with aldosterone by tail-cuff using the Visitech-2000 system. For mose experiments of cardiac miR-34a inhibition, C57BL/6J mice were locally injected with 1×10^{12} lentivirus endocind miR-34a sponge or control with cardiac-specific *Myh6* promoter for 14 days, then treated with aldosterone (50 μg/kg per day) by using osmotic pump for 21 days. Mice were peritoneally injected with dormicum (6.25 mg/kg) for euthanasia, then the blood and hearts were collected for further analysis. All animal experiments took place in the Shufeng Li's lab at Harbin Medical University.

Echocardiography analysis of cardiac function

All mice underwent echocardiographic measurement by using the Vevo 2100 system (Vevo). Echocardiographic parameters included heart rate, ejection fraction (EF), fractional shortening (FS), left ventricular anterior wall (LVAW),

left ventricular internal dimension (LVID), left ventricle posterior wall thickness (LVPW), and left ventricle mass (LV mass).

Histological analysis of cardiac tissues

Heart tissues were fixed in 4% paraformaldehyde for 48 h and embedded in paraffin. Five-micrometer-thick paraffin sections were prepared and stained with Hematoxylin and Eosin (H&E) solution. To investigate the histological changes, the cardiac images were observed under a light microscope (magnification ×100, Nikon, Tokyo). The average cardiomyocyte size was calculated in 20 cells/field (10 fields per mouse). For analyzing cardiac fibrosis, hydrated cardiac sections were stained with 0.1% SR F3B and 1.3% saturated aqueous solution of picric acid to evaluate the type IV collagen collection. The relative expression of collagen was measured by density analysis in captured images (magnification ×200, 10 fields per mouse). The calculation of histological analysis was done in a blinded fashion by two individuals.

Western blot analysis

Fifty micrograms of protein were run on 10% SDS/PAGE, and then transferred to a 0.22-μm polyvinylidene difluoride membrane (PVDF, Amersham Biosciences). The membrane was blocked for 1.5 h at room temperature with 10% milk in phosphate-buffered saline/0.05% Tween 20. The membrane was incubated overnight at 4°C with anti-TRIF, anti-TGF-β1, anti-SMAD3, anti-IRF3, or anti-Tubulin antibody and secondary antibodies (Cell Signaling, Danvers, MA). The protein expression was visualized using enhanced chemiluminescence reagents (Bio-Rad, Hercules, CA). The amounts of the proteins were analyzed using ImageJ analysis software version 1.38e.

Real-time quantitative PCR analysis

Total RNA in heart tissues or primary cardiomyocytes was extracted by using TRIzol (Invitrogen, Shanghai) according to the manufacturer's protocol. Reverse transcription was performed using the Superscript III Reverse Transcription System (Invitrogen), and real-time PCR analysis was performed using SYBR Green (Applied Biosystems, Alameda, CA). The sequence of primers were listed as following: *Trif*, forward 5′-AGGACAAACGCCGGAACTTTT-3′, reverse 5′-GCCGATAGTCTGTCTGTTCTAGT-3′; *Vdac1*, forward 5′- TGCCTCCCACATATGCTGATC-3′, reverse 5′-TCCGCCAGGGATGTCTT-3′; *Pgc1α*, forward 5′-GGACATGTGCAGCCAAGACTCT-3′, reverse 5′-CACTTCAATCCACCCAGAAAGCT-3′; *Nrf1*, forward 5′-GACCCAAACTGAACACATGGC-3′, reverse 5′-GTGCTCAGTGTACGTGGCTA-3′; *Tgf-β1*, forward 5′-CGCCTCTATGAGAAAACC-3′, reverse 5′-GTAACGCCAGGAATTGT-3′; *Col6α1*, forward 5′-GATGAGGGTGAAGTGGGAGA-3′, reverse 5′-CAGCACGAAGAGGATGTCAA-3′; *MMP12*, forward 5′-ACATTTCGCCTCTCTGCTGATGAC-3′, reverse 5′-CAGAAACCTTCAGCCAGAAGAACC-3′; *Anp*, forward 5′-GCCGGTAGAAGATGAGGTCA-3′, reverese 5′-AGCTGGATCTTCGTAGGCTC-3′; *Bnp*, forward 5′-GGCCTCACAAAAGAACACCC-3′, reverese 5′-TTACAGCCCAAACGACTGAC-3′; *Gapdh*, forward 5′-AGGAGCGAGACCCCACTAAC-3′, reverse 5′-GATGACCCTTTTGGCTCCAC-3′. The relative expression was normalized to *Gapdh*. For miRNA analysis, 200 ng RNA was reversed using the TaqMan MicroRNA Reverse Transcription Kit (Thermo Fisher), and real-time PCR analysis was performed using TaqMan Assay (Applied Biosystems). The relative expression of miR-34a was normalized to sno202.

Mitochondrial activity measurement

Cardiac ATP was measured using an ATP measurement kit (Molecular Probes, Carlsbad) [20]. The endogenous basal oxygen consumption was measured with a Clark electrode in a water-jacketed chamber connected to a circulating water bath (Hansatech, Norfolk, U.K.). The mitochondrial citrate synthase activity was measured by using Citrate Synthase Activity Assay Kit (Abcam, #ab119692).

Flow cytometry analysis of infiltrated immune cells

The cells from hearts were isolated by enzyme digestion [21]. Briefly, left ventricle was collected, and cut into small strips. Then the tissue was placed in a digestion buffer containing 1.5 mg/ml of Collagenase A (Roche) and 0.4 mg/ml DNaseI (Roche) in HBSS plus 5% fetal bovine serum and 10 mM HEPES. After two-round digestion, the cells were extracted by centrifuge. For toxic T analysis, the cells were stained with anti-Cd45 and anti-Cd3 antibodies. For macrophage analysis, the cells were stained with anti-Cd11b and anti-F4/80 antibodies. The result was recorded by calculating the positive cells in 10^5 heart cells.

Clinical Science (2020) **134** 1319–1331
https://doi.org/10.1042/CS20200249

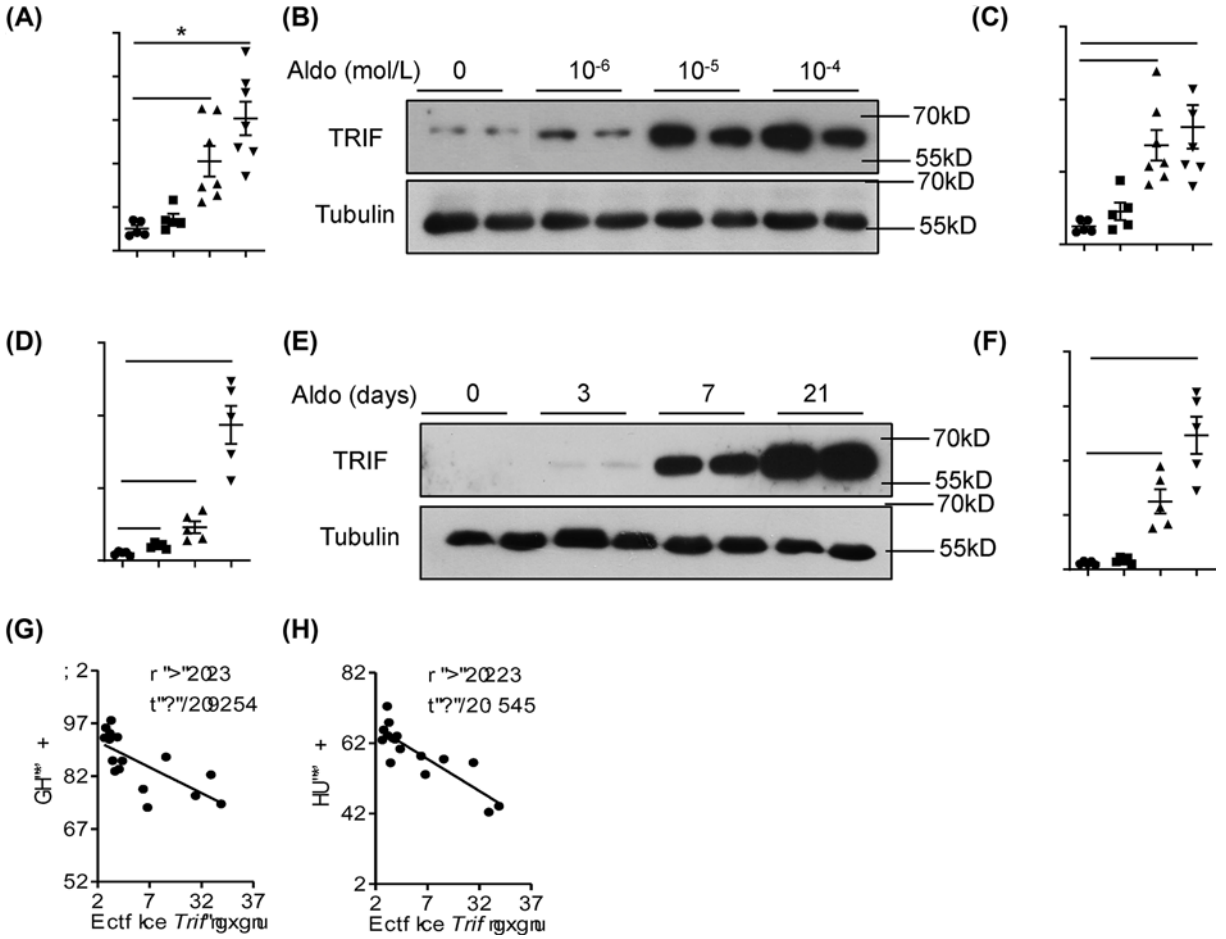

Figure 1. The aldosterone-induced TRIF level was positively correlated with cardiac dysfunction

(**A–C**) A total of 1 × 10^6 mouse primary cardiomyocytes were treated with different concentration (0, 10^{-6}, 10^{-5}, 10^{-4} mol/l) of aldosterone (Aldo) for 24 h. Real-time PCR analysis of *Trif* level (A), and immunoblot analysis of TRIF (B) and quantitative analysis of relative protein expression (C). (**D**,**E**) Male C57BL/6N mice were treated with aldosterone (50 μg/kg per day) by using osmotic pump for 0, 3, 7 and 21 days. Real-time PCR analysis of *Trif* level (D), and immunoblot analysis of TRIF (E) and quantitative analysis of relative protein expression (**F**). (**G**,**H**). Echocardiographic analysis of mouse cardiac EF and FS. Correlation between cardiac gene level of *Trif* and EF (G) and FS (H). Results were shown as mean ± SEM, and n=5–7 independent experiments or 5 mice/group. *P<0.05, **P<0.01, ***P<0.001.

Statistical analysis

Data were presented as mean ± SD. Student's t test was used for comparing two groups, and one-way ANOVA was used for comparing multiple groups. GraphPad Prism 5 (GraphPad, San Diego, CA) was used to analyze the statistical significance between sets of data. Differences were considered to be significant at P<0.05.

Results

Cardiac TRIF participates in aldosterone-induced cardiac dysfunction

Aldosterone, one of the end products of RAAS signaling, has multiple biological effects in cardiovascular remodeling [4]. In pathophysiological process, aldosterone causes inflammation leading to fibrosis and remodeling in the heart and vasculature [5–7]. TLR4 is involved in aldosterone-induced cardiac and kidney injuries [22]. Therefore, we further explored the possible role of TRIF in aldosterone-mediated cardiac remodeling. In primary mouse cardiomyocytes, aldosterone dose-dependently increased expression of *Trif* (Figure 1A) and TRIF protein levels (Figure 1B,C). Furthermore, mice were treated with aldosterone for 0, 3, 7, and 21 days. As Figure 1D–F showed, aldosterone also time-dependently increased cardiac expression of *Trif* (Figure 1D) and TRIF protein levels (Figure 1E,F). Chronic

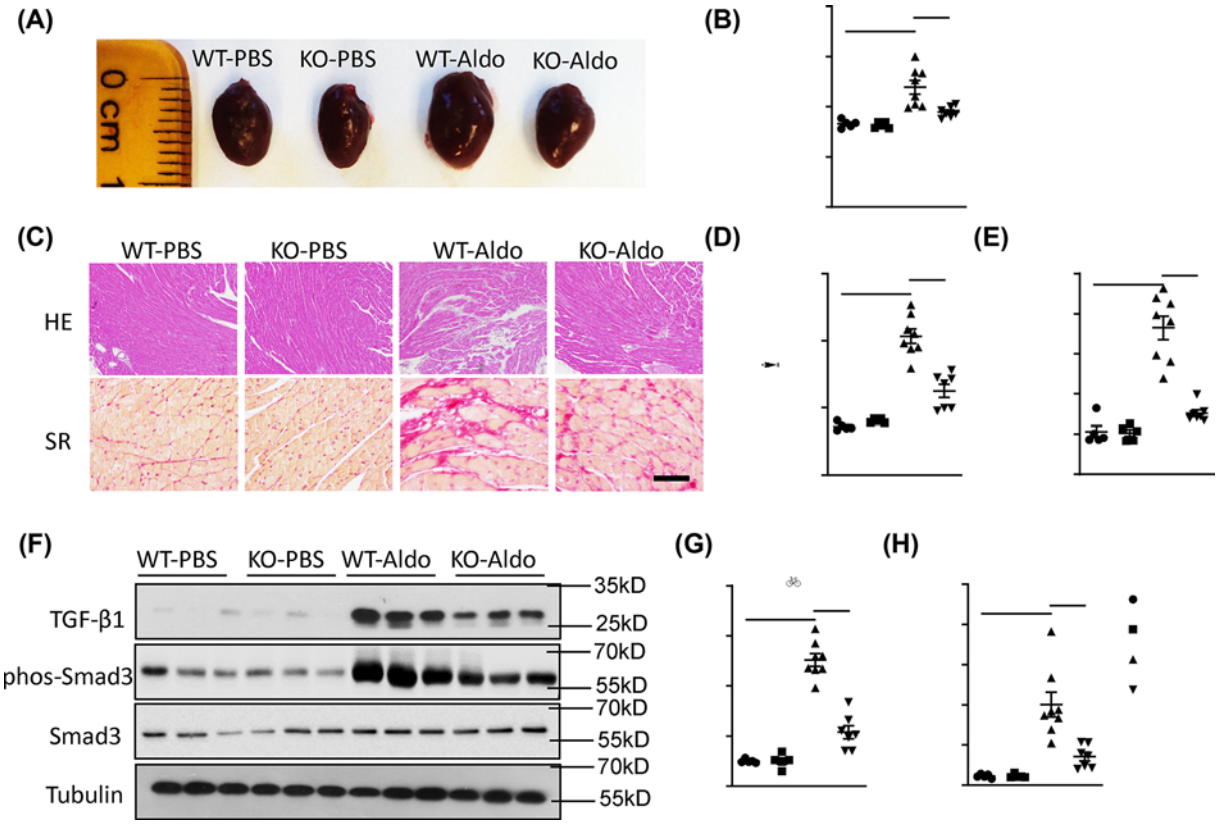

Figure 2. Trif deficiency protects against aldosterone-induced mouse cardiac hypertrophy and fibrosis

Trif knockout and wild-type mice were treated with aldosterone (50 μg/kg per day) by using osmotic pump for 21 days. (**A**) Representative image of hearts. (**B**) The ratio of heart weight/tibia length. (**C**–**E**) Cardiac slides were stained with H&E or SR staining solution (C), quantitative analysis of average cardiomyocyte size (D), and relative density of collagen (E). Scale bar = 100 μm. (**F**–**H**) Immunoblot analysis of TGF-β1, phos-SMAD3, and SMAD3 (F), and quantitative analysis of the relative density of TGF-β1/Tubulin (G) and phos-SMAD3/SMAD3 (H). Results were shown as mean ± SEM, and n=5–8 mice/group. *P<0.05, **P<0.01, ***P<0.001.

higher level of aldosterone impaired cardiac function, including reduction in EF and FS [23]. Interestingly, as Figure 1G,H showed, the increasing level of cardiac *Trif* was negatively correlated with EF ($r = -0.7032$, $P<0.01$) and FS ($r = -0.8323$, $P<0.001$). These results indicated up-regulation of cardiac TRIF might modulate aldosterone-induced cardiac dysfunction.

TRIF deficiency protects against aldosterone-induced cardiac hypertrophy, fibrosis, inflammatory response, and mitochondrial dysfunction

To identify the role of TRIF in aldosterone-induced cardiac remodeling, we next treated TRIF knockout mice with aldosterone for 21 days. As shown in Figure 2A,B, aldosterone-induced cardiac enlargement (Figure 2A), and increased the ratio of heart weight/tibia length (Figure 2B, $P<0.001$). Consistently, aldosterone also increased the average size of cardiomyocytes (Figure 2C,D, $P<0.001$). However, TRIF deficiency attenuated aldosterone-induced cardiac hypertrophy, heart weight/tibia length ratio and average cell size (Figure 2A–D, $P<0.01$). A variety of studies have demonstrated that cardiac remodeling was affected by several essential factors, including ANP, BNP, and myosin heavy chain (MHC) [24–26]. Therefore, we detected the expression of these markers in heart tissues. As showed in Supplementary Figure S1A–C, Trif deficiency effectively decreased aldosterone-induced cardiac levels of ANP, BNP, and MHC. Furthermore, aldosterone induced more severe cardiac injuries in 42 days (Supplementary Figure S2A–C), but TRIF deficiency effectively reversed aldosterone-induced cardiac hypertrophy. Tissue fibrosis is one of key characters in cardiac remodeling [27]. SR) stainin showed aldosterone obviously accumulated collagen deposit in hearts (Figure 2C,E, $P<0.001$), whereas TRIF deficiency reversed this up-regulation (Figure 2C,E, $P<0.01$). Then,

Clinical Science (2020) **134** 1319–1331
https://doi.org/10.1042/CS20200249

Table 1 The echocardiographic analysis of cardiac parameters in mice after treated with aldosterone for 21 days

	WT-PBS	KO-PBS	WT-Aldo	KO-Aldo
Heart rate (beats/min)	471 ± 34[1]	460 ± 22[1]	499 ± 59	479 ± 17[1]
EF%	75.54 ± 9.33[2]	77.32 ± 11.76[2]	50.11 ± 10.34	69.32 ± 6.32[2]
FS%	48.12 ± 5.43[2]	49.12 ± 9.01[2]	32.54 ± 9.03	43.12 ± 6.02[1]
LVAW;d (mm)	0.87 ± 0.11[3]	0.85 ± 0.21[3]	1.34 ± 0.26	0.96 ± 0.14[2]
LVAW;s (mm)	1.12 ± 0.20[3]	1.05 ± 0.19[3]	1.68 ± 0.33	1.35 ± 0.21[1]
LVID;d (mm)	3.64 ± 0.09[2]	3.32 ± 0.18[2]	4.42 ± 0.38	3.80 ± 0.45[1]
LVID;s (mm)	2.11 ± 0.16[1]	2.22 ± 0.17[1]	2.79 ± 0.31	2.33 ± 0.19[1]
LVPW;d (mm)	0.69 ± 0.21[3]	0.63 ± 0.17[3]	1.14 ± 0.27	0.82 ± 0.29[1]
LVPW;s (mm)	1.09 ± 0.23[2]	1.11 ± 0.12[2]	1.56 ± 0.25	1.23 ± 0.18[1]
LV mass (mg)	114.32 ± 9.33[3]	113.44 ± 15.03[3]	181.99 ± 26.42	132.07 ± 21.23[2]

Data are means ± SEM.
[1]$P<0.05$.
[2]$P<0.01$.
[3]$P<0.001$, as compared with WT-Aldo group.

we measured the fibrotic signaling. As showed in Figure 2E–G, aldosterone significantly increased the expression of TGF-β1 and phos-SMAD3 in wild-type mice ($P<0.001$). TRIF deficient mice exhibited an effective reduction of fibrotic protein levels (Figure 2E–G, $P<0.001$). Furthermore, cardiac functional measurement showed TRIF deficiency increased the levels of EF and FS, but reduced left ventricle wall thickness and left ventricle mass, as compared with aldosterone-treated wild-type mice for 21 or 42 days (Table 1 and Supplementary Table S1).

Aldosterone is a strong inducer of cardiovascular inflammation, with the help of TLR4 signaling [22]. To this end, we analyzed the downstream signaling of TLR4 cofactor TRIF in aldosterone-treated mice. TRIF could activate IRF3 in a phosphorylation-dependent manner, and transduce the inflammatory signaling [28]. Consistently, aldosterone remarkably increased the expression of cardiac phos-IRF3 (Figure 3A,B), downstream IFN-α (Figure 3C and Supplementary Figure S2D, $P<0.001$), and inflammatory cytokines TNF-α (Figure 3D and Supplementary Figure S2E, $P<0.001$), IL-1β (Figure 3E and Supplementary Figure S2F, $P<0.001$), and nitric oxide (Figure 3F and Supplementary Figure S2G, $P<0.001$) on days 21 and 42. In contrast, cardiac deficiency of TRIF significantly decreased aldosterone-induced phos-IRF3 and the production of inflammatory cytokines (Figure 3A–F). Furthermore, we measured the local expression of cardiac IFN-α by immunofluorescence staining. As shown in Supplementary Figure S3A,B, IFN-α was highly localized in aldosterone-treated WT mice ($P<0.001$), but TRIF deficiency suppressed this up-regulation ($P<0.001$). Flow cytometry analysis further supported TRIF deficiency attenuated aldosterone-induced cardiac inflammatory response by decreasing the percentage of F4/80+ macrophages (Supplementary Figure S3C, $P<0.001$) and $Cd3^+$ toxic T cells (Supplementary Figure S3D, $P<0.01$). Previous studies have demonstrated that aldosterone can elevate blood pressure, which contributes to cardiac remodeling [29,30]. As shown in Supplementary Figure S4, aldosterone obviously increased systolic blood pressure on days 7 and 21 ($P<0.01$). However, TRIF deficiency had no significant effects on blood pressure in WT or KO mice.

Mitochondrial biogenesis and activities determine cardiac metabolism and the response to foreign stimuli. Ibarrola et al. reported that aldosterone impaired cardiac mitochondrial function in human myocardial biopsies [31]. Similarly, present study also found aldosterone decreased the levels of mitochondrial biogenesis genes, including *Vdac1*, *Pgc1α*, and *Nrf1* (Figure 3G), but TRIF deficiency could significantly reverse this down-regulation (Figure 3G, $P<0.05$). Furthermore, aldosterone also inhibited cardiac mitochondrial activities, including ATP production (Figure 3H, $P<0.01$), oxygen consumption (Figure 3I, $P<0.001$) and citrate synthase activity (Figure 3J, $P<0.001$). However, TRIF deficiency effectively maintained the mitochondrial activities in aldosterone-treated mice (Figure 3H–J, $P<0.05$). Taken together, these results determined TRIF played a critical role in aldosterone-induced cardiac remodeling.

Cardiac miR-34a mediates the physiological role of aldosterone/TRIF in cardiac remodeling

Amounts of studies have found miR-34a existed crucial roles in cardiac aging, proliferation, and immune response [32–34]. However, it was unknown whether miR-34a participated in aldosterone-induced cardiac remodeling. Here, we found aldosterone dose-dependently increased the expression of miR-34a in primary mouse cardiomyocytes

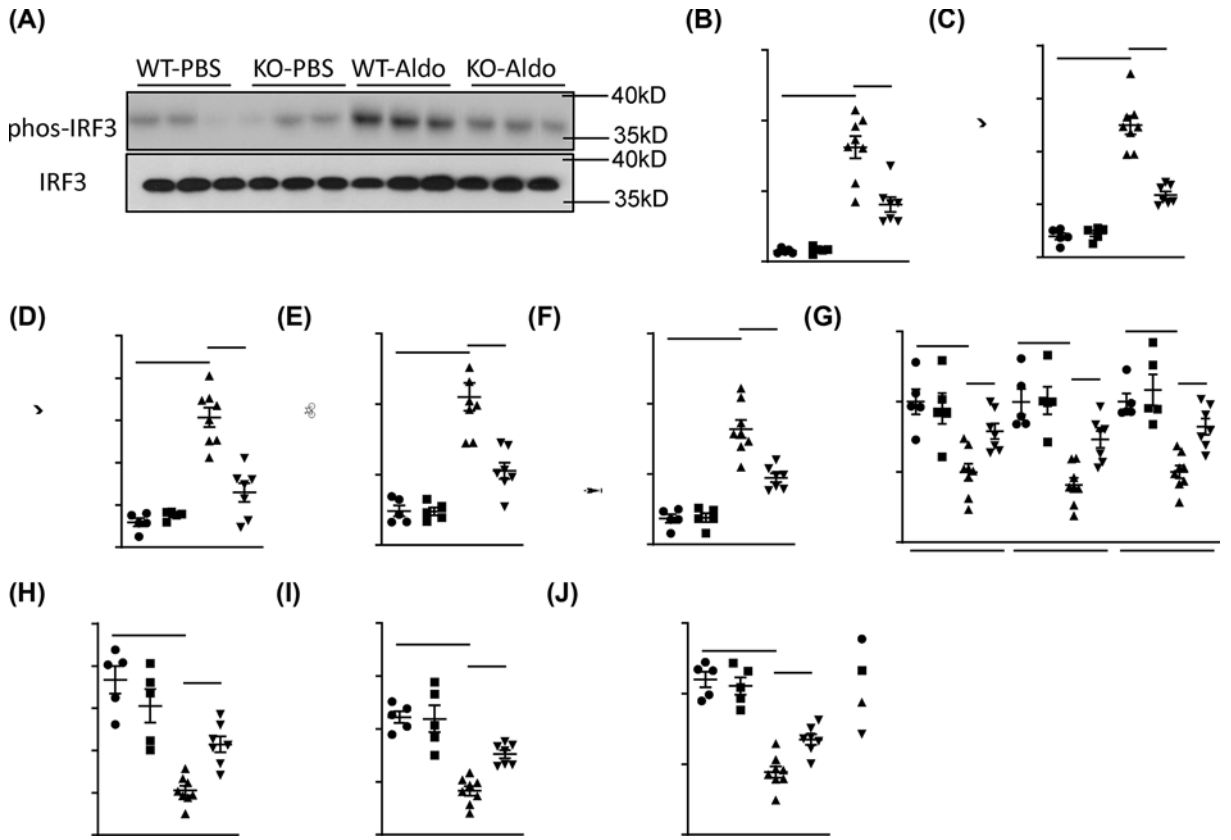

Figure 3. Trif deficiency attenuates aldosterone-induced cardiac inflammatory response and mitochondrial dysfunction

(**A**,**B**) Immunoblot analysis of IRF-3 (A), and quantitative analysis of the relative density of IRF-3/Tubulin (B). (**C–F**) Cardiac lysates were measured by kits for IFN-α (C), TNF-α (D), IL-1β (E), and nitric oxide (F) levels. (**G**) The mitochondrial gene levels of *Vdac1*, *Pgc1*α, and *Nrf1* in hearts. (**H–J**) Extracted cardiac mitochondria were measured for relative ATP level (H), oxygen consumption (I), and citrate synthase activity (J). Results were shown as mean $\pm$ SEM, and n=5–8 mice/group. $^{*}P<0.05$, $^{**}P<0.01$, $^{***}P<0.001$.

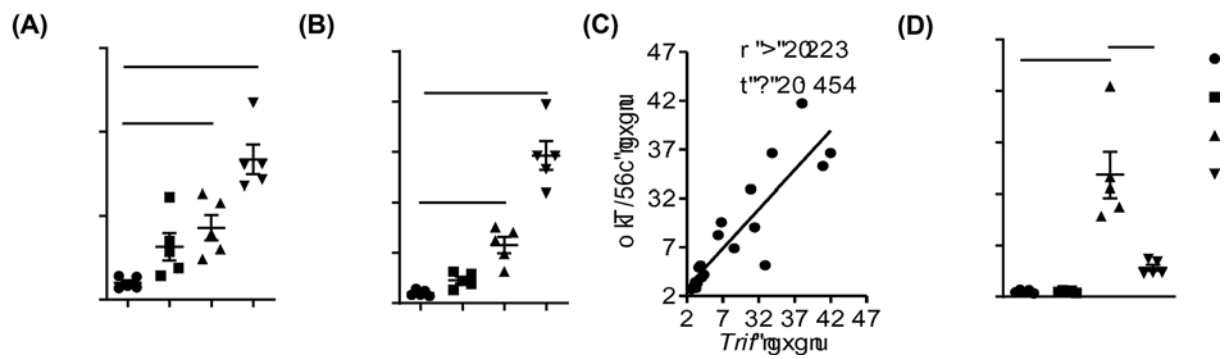

Figure 4. The elevated level of cardiac miR-34a closely correlates with Trif expression in aldosterone-treated mice

(**A**) A total of 1 $\times$ 10^6 mouse primary cardiomyocytes were treated with different concentrations (0, 10^{-6}, 10^{-5}, 10^{-4} mol/l) of aldosterone (Aldo) for 24 h. Real-time PCR analysis of miR-34a level. (**B**,**C**) Male C57BL/6N mice were treated with aldosterone (50 μg/kg per day) by using osmotic pump for 0, 3, 7, and 21 days. Real-time PCR analysis of miR-34a level (B), and the correlation between miR-34a level and cardiac *Trif* levels (C). (**D**) Trif knockout and wild-type mice were treated with aldosterone (50 μg/kg per day) by using osmotic pump for 21 days. The cardiac expression of miR-34a. Results were shown as mean $\pm$ SEM, and n=5 independent experiments or 5 mice/group. $^{*}P<0.05$, $^{**}P<0.01$, $^{***}P<0.001$.

(Figure 4A), and time-dependently stimulated miR-34a levels in mouse hearts (Figure 4B). More importantly, aldosterone downstream inflammatory molecules, such as IFN-α, TNF-α, and IL-1β, dose-dependently increased

Clinical Science (2020) **134** 1319–1331
https://doi.org/10.1042/CS20200249

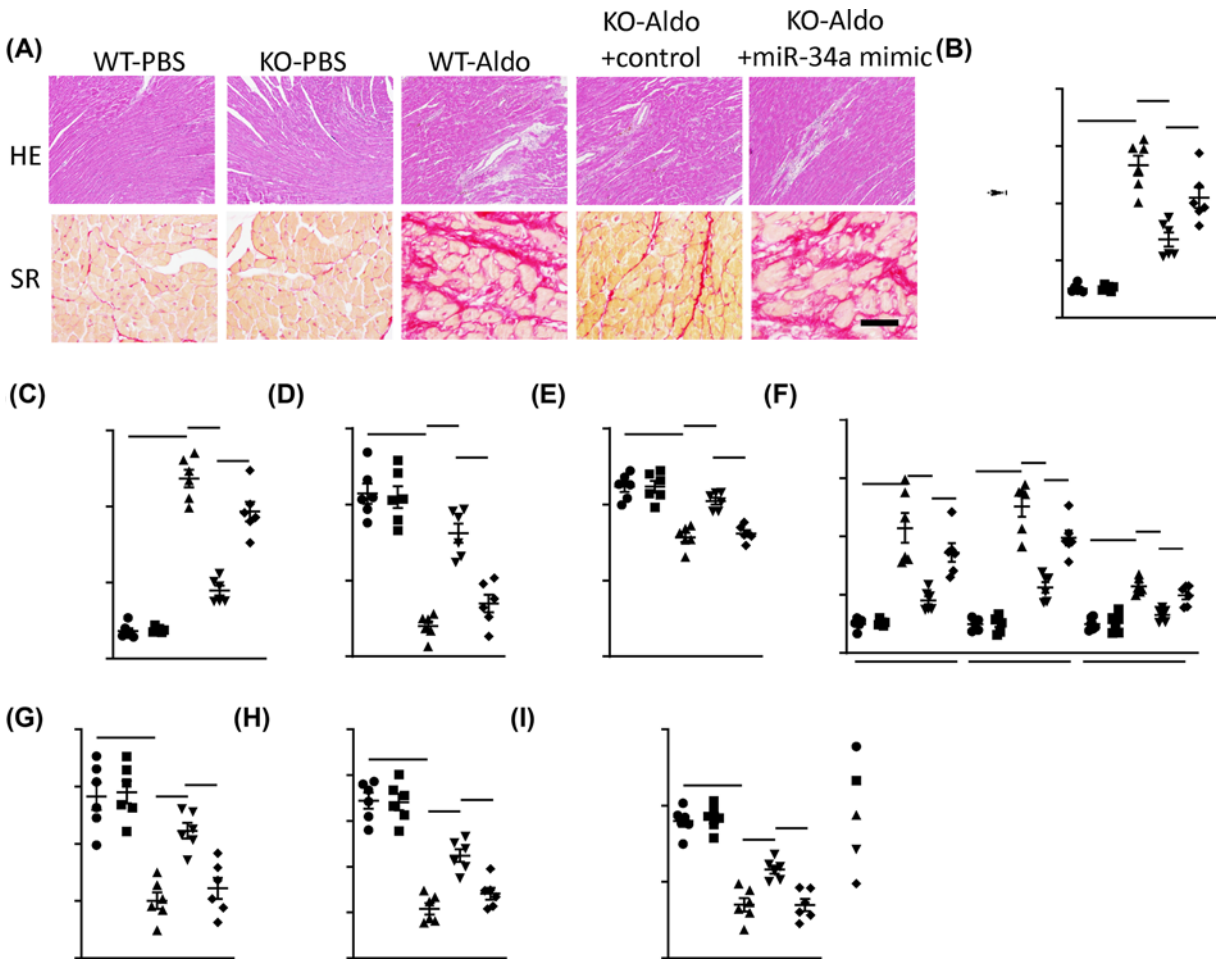

Figure 5. MiR-34a modulates Trif-mediated cardiac remodeling in aldosterone-treated mice

Trif knockout mice were administrated with 1 × 10^9 AAV encoding miR-34a mimic or control with cardiac-specific *Myh6* promoter for 14 days, then treated with aldosterone (50 μg/kg per day) by using osmotic pump for 21 days. (**A–C**) Cardiac slides were stained with H&E or SR staining solution (A), and quantitative analysis of average cardiomyocyte size (B) and relative density of collagen (C). Scale bar = 100 μm. (**D**,**E**) Echocardiographic analysis of mouse cardiac EF (D) and FS (**E**). (**F**) The fibrotic gene levels of *Tgf-β1*, *Col6α1* and *Mmp12*. (**G–I**) Extracted cardiac mitochondria were measured for relative ATP level (G), oxygen consumption (H), and citrate synthase activity (I). Results were shown as mean ± SEM, and n=6 mice/group. *P<0.05, **P<0.01, ***P<0.001.

miR-34a levels in cardiomyocytes (Supplementary Figure S5A–C). The incremental up-regulation of cardiac miR-34a was also positively correlated with *Trif* levels (Figure 4C, r = 0.8232, P<0.001). More importantly, the up-regulated level of miR-34a was obviously decreased in aldosterone-treated TRIF deficient mice (Figure 4D, P<0.01).

To identify the role of miR-34a in aldosterone-induced cardiac remodeling, we next utilized the AAV to specifically overexpress cardiac miR-34a in TRIF-deficient mice. As shown in Supplementary Figure S6, the decreased cardiac miR-34a was obviously reversed in TRIF-deficient mice treated with AAV encoding miR-34a mimic (P<0.001). Interestingly, replenishment of cardiac miR-34a abolished the cardiac benefits, including enlargement of cardiomyocyte size (Figure 5A,B, P<0.05), induction of collagen deposits (Figure 5A,C, P<0.01), and impaired cardiac function (Figure 5D,E, P<0.05), as compared with aldosterone-treated TRIF-deficient mice. The expression fibrotic genes, such as *Tgf-β1*, *Col6α1*, and *Mmp12*, were remarkably increased in miR-34a mimic-treated mice (Figure 5F, P<0.05). Besides, the mitochondrial protection of TRIF deficiency was also partially abolished after miR-34a overexpression. In details, overexpression of cardiac miR-34a decreased ATP production (Figure 5G, P<0.05), oxygen consumption (Figure 5H, P<0.05) and citric synthase activity (Figure 5I, P<0.05).

On the contrast, specific inhibition of cardiac miR-34a attenuated aldosterone-induced cardiac hypertrophy (Supplementary Figure S7A,B, P<0.01). SR staining showed miR-34a sponge decreased cardiac collagen accumulation in

aldosterone-treated mice (Supplementary Figure S7A,C, $P<0.01$). Similarly, cardiac functional measurement showed miR-34a sponge increased the levels of EF and FS, as compared with aldosterone-treated mice (Supplementary Figure S7D,E). MiR-34a sponge also improved cardiac mitochondrial activities, including ATP production (Supplementary Figure S7F, $P<0.05$), oxygen consumption (Supplementary Figure S7G, $P<0.01$), and citrate synthase activity (Supplementary Figure S7H, $P<0.05$). All these findings supported cardiac miR-34a partially determined aldosterone/TRIF-mediated cardiac remodeling.

Discussion

Abnormal activation of RAAS, including a higher level of aldosterone, has been demonstrated to trigger an inflammatory process in cardiovascular diseases [4]. In aldosterone-treated rats, there was a significant induction of inflammatory response in hearts [6,7]. A recent study found deletion of MR, known as the aldosterone receptor, markedly reduced the cardiac inflammation, fibrosis, and functional disorders in deoxycorticosterone acetate/salt-treated animals [35]. The present study aimed to identify the role of TRIF, a critical inflammatory regulator, in aldosterone-induced cardiac remodeling and the molecular mechanisms. Through utilizing TRIF-deficient mouse model, we found TRIF determined aldosterone-induced cardiac remodeling, including cardiac hypertrophy, functional disorders, fibrosis, inflammatory response, and mitochondrial injuries. Mechanistically, the incremental increasing miR-34a was a potential mediator in aldosterone/TRIF-induced heart damages. Cardiac special overexpression of miR-34a abolished the cardioprotective profiles in TRIF-deficient mice, whereas miR-34a inhibition could attenuate aldosterone-induced abnormal cardiac remodeling. Taken together, TRIF/miR-34a axis mediated aldosterone-induced cardiac remodeling.

Multiple factors are contributed to the process of cardiac remodeling leading to cardiac functional disorders and further heart failure. Excess activation of adrenergic signaling and/or RAAS are major molecular pathways triggering cardiovascular changes. The circulating levels of aldosterone were closely correlated with the increasing incidence of cardiovascular diseases [36]. In patients with severe heart failure, there were extremely higher levels of circulating aldosterone [8,37]. Beygui et al. found that plasma aldosterone levels were quickly increased to more than two-fold after myocardial infarction, and precisely predicted the therapeutic outcomes [38].In obese mice, plasma levels of aldosterone were also obviously elevated [39,40]. Blockage of aldosterone signaling had therapeutic benefits in protecting against heart failure and related cardiovascular complications [8,37].

Although it was well-established that aldosterone closely linked to cardiac remodeling, mechanisms by how aldosterone affected cardiac pathophysiological process remained unclear. One of the key contributors was aldosterone-induced cardiac inflammatory response. Aldosterone triggered excess production of reactive oxygen species (ROS) and inflammatory cytokines, whereas blockage of TLR 4 could reverse cardiac hypertrophy, dysfunction, and inflammatory response [22]. As one of necessary adaptors in TLR4 complex, TRIF is another critical mediator of signaling cascades that directly influences multiple cellular processes [15]. For example, stimulation of TRIF activates NF-κB and MAPK pathways that trigger transcription of numerous inflammatory cytokines [41,42]. Previous studies have reported TRIF-mediated inflammatory cascades led to oxidative stress, cardiac hypertrophy, and cellular apoptosis after myocardial infarction [43]. Present echocardiographic results showed cardiac TRIF was a critical mediator in aldosterone-induced cardiac hypertrophy. As an inflammatory transducer, this finding supported the close links between excessive inflammatory response and cardiac hypertrophy. Pathological hypertrophy is often characterized as impaired myocardial vascularization, unfavorable changes in the extracellular matrix composition, and fibrosis [44]. The abnormal inflammatory response, such as increased levels of TNF-α and soluble TNF-α receptors, serves as prognostic markers in patients with heart hypertrophy [45]. In present study, TRIF deficiency not only significantly reduced aldosterone-induced cardiac inflammation, but also improved cardiac hypertrophy.

A variety of studies have demonstrated that aldosterone and the MR antagonists modulate cardiac hypertrophy [46–48]. Aldosterone also directly promoted cardiomyocyte hypertrophy and induced the expression of fetal-type cardiac genes *in vitro* in a manner dependent on activation of the MR. In present study, the expression of cardiac hypertrophic markers, including ANP, BNP, and MHC, was significantly decreased in Trif KO mice treated with aldosterone. Furthermore, aldosterone has been demonstrated to influence cardiac remodeling independent of its impact on systemic blood pressure, whereas cardiac fibrosis could be prevented by treatment with non-antihypertensive doses of spironolactone [44,49]. These reported findings were consistent to our present results. The Trif KO had no significant effect on blood pressure, but suppressed cardiac expression of fibrotic genes and protein. Therefore, although our results had not provided a completely new mechanism in MR activation-induced myocardial hypertrophy, we first addressed the novel role of aldosterone/Trif/miR-34a signaling in cardiac remodeling.

Clinical Science (2020) **134** 1319–1331
https://doi.org/10.1042/CS20200249

Previous studies have also demonstrated that aldosterone could regulate the cardiac expression of miR levels. In neonatal rat cardiomyocytes, aldosterone-induced cell hypertrophy concurred with up-regulation of miR-23a level [50]. Aldosterone down-regulated the expression of miR-208b, which suppressed β-myosin heavy chain transcription [51]. Syed et al. found miR-21 deficiency exacerbated aldosterone-mediated cardiac abnormal remodeling and dysfunction [12]. In the present study, we first provided evidence that cardiac miR-34a was also increased in aldosterone-treated primary mouse cardiomyocytes and heart tissues. MiR-34a is one of the most widely studied miRNAs in mammalian cells due to its critical role in the pathophysiology of multiple phenotypes such as solid tumors, cardiac injury, and tissue inflammation [32,34,52]. In several cardiovascular diseases, miR-34a exacerbated cardiac aging, suppressed cardiac repair and regeneration following myocardial infarction, and positively correlated with the incidence of cardiovascular diseases [32,33,53]. Mechanistically, miR-34a stimulated tissue inflammation through repressing transcriptional factors, such as Kruppel-like factor (KLF) 4 and sirtuin (SIRT) 1 [34,54]. Consistently, our present findings showed that overexpression of cardiac miR-34a abolished the anti-inflammatory effects of TRIF deficiency, and maintained the pro-inflammatory profiles of aldosterone in hearts. It will be meaningful to maintain cardiac structure and function through blocking TRIF/miR-34a axis.

The present study first addressed the existence of cardiac TRIF/miR-34a signaling, which mediated the pathophysiological role of aldosterone in cardiac remodeling. However, the detailed molecular interaction between these two targets was still unclear. Our finding supposed TRIF downstream inflammatory factors were possible mediators. In a future study, it needs to fully investigate the underlying mechanism.

In conclusion, the present study supported TRIF was a potential therapeutic target for cardiac pathophysiological remodeling. The TRIF/miR-34a axis could provide a novel molecular mechanism for explaining aldosterone-induced cardiac hypertrophy, fibrosis, and dysfunction.

Clinical perspectives

- Aldosterone, as a major product of RAAS, deteriorates the pathophysiological process of myocardial injuries through affecting multiple signaling in clinical studies. Among them, TRIF signaling-mediated cardiac inflammatory response is one of key factors in determining cardiac remodeling. Aldosterone obviously increased the cardiac levels of TRIF, which was closely correlated with cardiac dysfunction. However, it was unknown whether or how cardiac TRIF mediated aldosterone-induced cardiac remodeling.

- Aldosterone antagonists have significant therapeutic benefits in patients with cardiac disorders. Therefore, we explored the roles of TRIF in aldosterone-induced cardiac injuries by utilizing TRIF genetic-deficient mice. TRIF deficiency protected against aldosterone-induced cardiac remodeling. Mechanistically, miR-34a participated in aldosterone/TRIF signaling, and specific overexpression of cardiac miR-34a abolished the cardiac benefits of TRIF deficiency in aldosterone-treated mice.

- Cardiac TRIF/miR-34a provided an explanation for the pharmacological benefits of aldosterone antagonists in cardiac injuries, and both cardiac TRIF and miR-34a might become the potential therapeutic targets.

Competing Interests

The authors declare that there are no competing interests associated with the manuscript.

Funding

This work was supported by the National Natural Science Foundation of China [grant number 81800362]; and the Young and Middle-aged Innovation Science Foundation from Second Affiliated Hospital of Harbin Medical University [grant number KYCX2018-24].

Author Contribution

S.j.L. conducted the mouse experiments, analyzed data, and discussed the results. W.C. conducted the primary cell experiments and analyzed data. B.W. and E.Z. conducted the osmotic pump implantation. J.X. discussed the results. S.f.L. guided all procedures, discussed the results, and wrote the manuscript.

Acknowledgements

The authors thank Dr. Qian Ni (Tianjin University) for gifting the viruses.

Abbreviations

AAV, adeno-associated virus; ANP, atrial natriuretic peptide; ATP, adenosine triphosphate; BNP, brain natriuretic peptide; EF, ejection fraction; FS, fractional shortening; IRF, IFN regulatory factor; LVID, left ventricular internal dimension; MHC, myosin heavy chain; miR, microRNA; MR, mineralocorticoid receptor; MyD88, myeloid differentiation primary response 88; *Myh6*, cardiac-specific α myosin-heavy chain; phos, phosphorylated; RAAS, renin–angiotensin–aldosterone system; SR, Sirius Red; TLR, Toll-like receptor; Trif/TRIF, TIR-domain-containing adapter-inducing interferon-β.

References

1 Orsborne, C., Chaggar, P.S., Shaw, S.M. and Williams, S.G. (2017) The renin-angiotensin-aldosterone system in heart failure for the non-specialist: the past, the present and the future. *Postgrad. Med. J.* **93**, 29–37, https://doi.org/10.1136/postgradmedj-2016-134045
2 Emdin, C.A., Callender, T., Cao, J., McMurray, J.J. and Rahimi, K. (2015) Meta-analysis of large-scale randomized trials to determine the effectiveness of inhibition of the renin-angiotensin aldosterone system in heart failure. *Am. J. Cardiol.* **116**, 155–161, https://doi.org/10.1016/j.amjcard.2015.03.052
3 Martin, N., Manoharan, K., Thomas, J., Davies, C. and Lumbers, R.T. (2018) Beta-blockers and inhibitors of the renin-angiotensin aldosterone system for chronic heart failure with preserved ejection fraction. *Cochrane Database. Syst. Rev.* **6**, CD012721
4 Weber, K.T. (2001) Aldosterone in congestive heart failure. *N. Engl. J. Med.* **345**, 1689–1697, https://doi.org/10.1056/NEJMra000050
5 Robert, V., Silvestre, J.S., Charlemagne, D., Sabri, A., Trouve, P., Wassef, M. et al. (1995) Biological determinants of aldosterone-induced cardiac fibrosis in rats. *Hypertension* **26**, 971–978, https://doi.org/10.1161/01.HYP.26.6.971
6 Rocha, R., Rudolph, A.E., Frierdich, G.E., Nachowiak, D.A., Kekec, B.K., Blomme, E.A. et al. (2002) Aldosterone induces a vascular inflammatory phenotype in the rat heart. *Am. J. Physiol. Heart Circ. Physiol.* **283**, H1802–H1810, https://doi.org/10.1152/ajpheart.01096.2001
7 Sun, Y., Zhang, J., Lu, L., Chen, S.S., Quinn, M.T. and Weber, K.T. (2002) Aldosterone-induced inflammation in the rat heart: role of oxidative stress. *Am. J. Pathol.* **161**, 1773–1781, https://doi.org/10.1016/S0002-9440(10)64454-9
8 Pitt, B., Zannad, F., Remme, W.J., Cody, R., Castaigne, A., Perez, A. et al. (1999) The effect of spironolactone on morbidity and mortality in patients with severe heart failure. Randomized Aldactone Evaluation Study Investigators. *N. Engl. J. Med.* **341**, 709–717
9 Marney, A.M. and Brown, N.J. (2007) Aldosterone and end-organ damage. *Clin. Sci.* **113**, 267–278, https://doi.org/10.1042/CS20070123
10 Johar, S., Cave, A.C., Narayanapanicker, A., Grieve, D.J. and Shah, A.M. (2006) Aldosterone mediates angiotensin II-induced interstitial cardiac fibrosis via a Nox2-containing NADPH oxidase. *FASEB J.* **20**, 1546–1548, https://doi.org/10.1096/fj.05-4642fje
11 Ahokas, R.A., Warrington, K.J., Gerling, I.C., Sun, Y., Wodi, L.A., Herring, P.A. et al. (2003) Aldosteronism and peripheral blood mononuclear cell activation: a neuroendocrine-immune interface. *Circ. Res.* **93**, e124–e135, https://doi.org/10.1161/01.RES.0000102404.81461.25
12 Syed, M., Ball, J.P., Mathis, K.W., Hall, M.E., Ryan, M.J., Rothenberg, M.E. et al. (2018) MicroRNA-21 ablation exacerbates aldosterone-mediated cardiac injury, remodeling, and dysfunction. *Am. J. Physiol. Endocrinol. Metab.* **315**, E1154–E1167, https://doi.org/10.1152/ajpendo.00155.2018
13 Robertson, S., MacKenzie, S.M., Alvarez-Madrazo, S., Diver, L.A., Lin, J., Stewart, P.M. et al. (2013) MicroRNA-24 is a novel regulator of aldosterone and cortisol production in the human adrenal cortex. *Hypertension* **62**, 572–578, https://doi.org/10.1161/HYPERTENSIONAHA.113.01102
14 Koyama, R., Mannic, T., Ito, J., Amar, L., Zennaro, M.C., Rossier, M.F. et al. (2018) MicroRNA-204 is necessary for aldosterone-stimulated T-type calcium channel expression in cardiomyocytes. *Int. J. Mol. Sci.* **19**, 2941, https://doi.org/10.3390/ijms19102941
15 Kenny, E.F. and O'Neill, L.A. (2008) Signalling adaptors used by Toll-like receptors: an update. *Cytokine* **43**, 342–349, https://doi.org/10.1016/j.cyto.2008.07.010
16 Singh, M.V., Cicha, M.Z., Meyerholz, D.K., Chapleau, M.W. and Abboud, F.M. (2015) Dual activation of TRIF and MyD88 adaptor proteins by angiotensin II evokes opposing effects on pressure, cardiac hypertrophy, and inflammatory gene expression. *Hypertension* **66**, 647–656, https://doi.org/10.1161/HYPERTENSIONAHA.115.06011
17 Antoniak, S., Cardenas, J.C., Buczek, L.J., Church, F.C., Mackman, N. and Pawlinski, R. (2017) Protease-activated receptor 1 contributes to angiotensin II-induced cardiovascular remodeling and inflammation. *Cardiology* **136**, 258–268, https://doi.org/10.1159/000452269
18 Li, W., Feng, G., Gauthier, J.M., Lokshina, I., Higashikubo, R., Evans, S. et al. (2019) Ferroptotic cell death and TLR4/Trif signaling initiate neutrophil recruitment after heart transplantation. *J. Clin. Invest.* **130**, 2293–2304, https://doi.org/10.1172/JCI126428
19 Pan, Y., Wang, Y., Zhao, Y., Peng, K., Li, W., Wang, Y. et al. (2014) Inhibition of JNK phosphorylation by a novel curcumin analog prevents high glucose-induced inflammation and apoptosis in cardiomyocytes and the development of diabetic cardiomyopathy. *Diabetes* **63**, 3497–3511, https://doi.org/10.2337/db13-1577
20 Nie, H., Pan, Y. and Zhou, Y. (2018) Exosomal microRNA-194 causes cardiac injury and mitochondrial dysfunction in obese mice. *Biochem. Biophys. Res. Commun.* **503**, 3174–3179, https://doi.org/10.1016/j.bbrc.2018.08.113

21 Yu, Y.R., O'Koren, E.G., Hotten, D.F., Kan, M.J., Kopin, D., Nelson, E.R. et al. (2016) A protocol for the comprehensive flow cytometric analysis of immune cells in normal and inflamed murine non-lymphoid tissues. *PLoS ONE* **11**, e0150606, https://doi.org/10.1371/journal.pone.0150606
22 Zhang, Y., Peng, W., Ao, X., Dai, H., Yuan, L., Huang, X. et al. (2015) TAK-242, a toll-like receptor 4 antagonist, protects against aldosterone-induced cardiac and renal injury. *PLoS ONE* **10**, e0142456, https://doi.org/10.1371/journal.pone.0142456
23 Cannavo, A., Liccardo, D., Eguchi, A., Elliott, K.J., Traynham, C.J., Ibetti, J. et al. (2016) Myocardial pathology induced by aldosterone is dependent on non-canonical activities of G protein-coupled receptor kinases. *Nat. Commun.* **7**, 10877, https://doi.org/10.1038/ncomms10877
24 Li, W., Fang, Q., Zhong, P., Chen, L., Wang, L., Zhang, Y. et al. (2016) EGFR inhibition blocks palmitic acid-induced inflammation in cardiomyocytes and prevents hyperlipidemia-induced cardiac injury in mice. *Sci. Rep.* **6**, 24580, https://doi.org/10.1038/srep24580
25 Feldman, A.M., Weinberg, E.O., Ray, P.E. and Lorell, B.H. (1993) Selective changes in cardiac gene expression during compensated hypertrophy and the transition to cardiac decompensation in rats with chronic aortic banding. *Circ. Res.* **73**, 184–192, https://doi.org/10.1161/01.RES.73.1.184
26 Battistoni, A., Rubattu, S. and Volpe, M. (2012) Circulating biomarkers with preventive, diagnostic and prognostic implications in cardiovascular diseases. *Int. J. Cardiol.* **157**, 160–168, https://doi.org/10.1016/j.ijcard.2011.06.066
27 Pan, Y., Zhu, G., Wang, Y., Cai, L., Cai, Y., Hu, J. et al. (2013) Attenuation of high-glucose-induced inflammatory response by a novel curcumin derivative B06 contributes to its protection from diabetic pathogenic changes in rat kidney and heart. *J. Nutr. Biochem.* **24**, 146–155, https://doi.org/10.1016/j.jnutbio.2012.03.012
28 Takeuchi, O. (2012) IRF3: a molecular switch in pathogen responses. *Nat. Immunol.* **13**, 634–635, https://doi.org/10.1038/ni.2346
29 Schmidt, B.M. and Schmieder, R.E. (2003) Aldosterone-induced cardiac damage: focus on blood pressure independent effects. *Am. J. Hypertens.* **16**, 80–86, https://doi.org/10.1016/S0895-7061(02)03199-0
30 Ruilope, L.M. (2008) Aldosterone, hypertension, and cardiovascular disease: an endless story. *Hypertension* **52**, 207–208, https://doi.org/10.1161/HYPERTENSIONAHA.108.111211
31 Ibarrola, J., Sadaba, R., Martinez-Martinez, E., Garcia-Pena, A., Arrieta, V., Alvarez, V. et al. (2018) Aldosterone impairs mitochondrial function in human cardiac fibroblasts via A-kinase anchor protein 12. *Sci. Rep.* **8**, 6801, https://doi.org/10.1038/s41598-018-25068-6
32 Boon, R.A., Iekushi, K., Lechner, S., Seeger, T., Fischer, A., Heydt, S. et al. (2013) MicroRNA-34a regulates cardiac ageing and function. *Nature* **495**, 107–110, https://doi.org/10.1038/nature11919
33 Yang, Y., Cheng, H.W., Qiu, Y., Dupee, D., Noonan, M., Lin, Y.D. et al. (2015) MicroRNA-34a plays a key role in cardiac repair and regeneration following myocardial infarction. *Circ. Res.* **117**, 450–459, https://doi.org/10.1161/CIRCRESAHA.117.305962
34 Pan, Y., Hui, X., Hoo, R.L.C., Ye, D., Chan, C.Y.C., Feng, T. et al. (2019) Adipocyte-secreted exosomal microRNA-34a inhibits M2 macrophage polarization to promote obesity-induced adipose inflammation. *J. Clin. Invest.* **129**, 834–849, https://doi.org/10.1172/JCI123069
35 Rickard, A.J., Morgan, J., Tesch, G., Funder, J.W., Fuller, P.J. and Young, M.J. (2009) Deletion of mineralocorticoid receptors from macrophages protects against deoxycorticosterone/salt-induced cardiac fibrosis and increased blood pressure. *Hypertension* **54**, 537–543, https://doi.org/10.1161/HYPERTENSIONAHA.109.131110
36 Vasan, R.S., Evans, J.C., Larson, M.G., Wilson, P.W., Meigs, J.B., Rifai, N. et al. (2004) Serum aldosterone and the incidence of hypertension in nonhypertensive persons. *N. Engl. J. Med.* **351**, 33–41, https://doi.org/10.1056/NEJMoa033263
37 Pitt, B., Remme, W., Zannad, F., Neaton, J., Martinez, F., Roniker, B. et al. (2003) Eplerenone, a selective aldosterone blocker, in patients with left ventricular dysfunction after myocardial infarction. *N. Engl. J. Med.* **348**, 1309–1321, https://doi.org/10.1056/NEJMoa030207
38 Beygui, F., Collet, J.P., Benoliel, J.J., Vignolles, N., Dumaine, R., Barthelemy, O. et al. (2006) High plasma aldosterone levels on admission are associated with death in patients presenting with acute ST-elevation myocardial infarction. *Circulation* **114**, 2604–2610, https://doi.org/10.1161/CIRCULATIONAHA.106.634626
39 Guo, C., Ricchiuti, V., Lian, B.Q., Yao, T.M., Coutinho, P., Romero, J.R. et al. (2008) Mineralocorticoid receptor blockade reverses obesity-related changes in expression of adiponectin, peroxisome proliferator-activated receptor-gamma, and proinflammatory adipokines. *Circulation* **117**, 2253–2261, https://doi.org/10.1161/CIRCULATIONAHA.107.748640
40 Nguyen Dinh Cat, A., Callera, G.E., Friederich-Persson, M., Sanchez, A., Dulak-Lis, M.G., Tsiropoulou, S. et al. (2018) Vascular dysfunction in obese diabetic db/db mice involves the interplay between aldosterone/mineralocorticoid receptor and Rho kinase signaling. *Sci. Rep.* **8**, 2952, https://doi.org/10.1038/s41598-018-21087-5
41 Palova-Jelinkova, L., Danova, K., Drasarova, H., Dvorak, M., Funda, D.P., Fundova, P. et al. (2013) Pepsin digest of wheat gliadin fraction increases production of IL-1beta via TLR4/MyD88/TRIF/MAPK/NF-kappaB signaling pathway and an NLRP3 inflammasome activation. *PLoS ONE* **8**, e62426, https://doi.org/10.1371/journal.pone.0062426
42 Pan, Y., Huang, Y., Wang, Z., Fang, Q., Sun, Y., Tong, C. et al. (2014) Inhibition of MAPK-mediated ACE expression by compound C66 prevents STZ-induced diabetic nephropathy. *J. Cell. Mol. Med.* **18**, 231–241, https://doi.org/10.1111/jcmm.12175
43 Chen, C., Feng, Y., Zou, L., Wang, L., Chen, H.H., Cai, J.Y. et al. (2014) Role of extracellular RNA and TLR3-Trif signaling in myocardial ischemia-reperfusion injury. *J. Am. Heart Assoc.* **3**, e000683, https://doi.org/10.1161/JAHA.113.000683
44 Weber, K.T. and Brilla, C.G. (1991) Pathological hypertrophy and cardiac interstitium. Fibrosis and renin-angiotensin-aldosterone system. *Circulation* **83**, 1849–1865, https://doi.org/10.1161/01.CIR.83.6.1849
45 Stork, T., Mockel, M., Danne, O., Voller, H., Eichstadt, H. and Frei, U. (1995) Left ventricular hypertrophy and diastolic dysfunction: their relation to coronary heart disease. *Cardiovasc. Drugs Ther.* **9**, 533–537, https://doi.org/10.1007/BF00877866
46 Takeda, Y., Yoneda, T., Demura, M., Miyamori, I. and Mabuchi, H. (2000) Sodium-induced cardiac aldosterone synthesis causes cardiac hypertrophy. *Endocrinology* **141**, 1901–1904, https://doi.org/10.1210/endo.141.5.7529
47 Qin, W., Rudolph, A.E., Bond, B.R., Rocha, R., Blomme, E.A., Goellner, J.J. et al. (2003) Transgenic model of aldosterone-driven cardiac hypertrophy and heart failure. *Circ. Res.* **93**, 69–76, https://doi.org/10.1161/01.RES.0000080521.15238.E5

48 Nagata, K., Obata, K., Xu, J., Ichihara, S., Noda, A., Kimata, H. et al. (2006) Mineralocorticoid receptor antagonism attenuates cardiac hypertrophy and failure in low-aldosterone hypertensive rats. *Hypertension* **47**, 656–664, https://doi.org/10.1161/01.HYP.0000203772.78696.67

49 Brilla, C.G., Matsubara, L.S. and Weber, K.T. (1993) Antifibrotic effects of spironolactone in preventing myocardial fibrosis in systemic arterial hypertension. *Am. J. Cardiol.* **71**, 12A–16A, https://doi.org/10.1016/0002-9149(93)90239-9

50 Lin, Z., Murtaza, I., Wang, K., Jiao, J., Gao, J. and Li, P.F. (2009) miR-23a functions downstream of NFATc3 to regulate cardiac hypertrophy. *Proc. Natl. Acad. Sci. U.S.A.* **106**, 12103–12108, https://doi.org/10.1073/pnas.0811371106

51 Azibani, F., Devaux, Y., Coutance, G., Schlossarek, S., Polidano, E., Fazal, L. et al. (2012) Aldosterone inhibits the fetal program and increases hypertrophy in the heart of hypertensive mice. *PLoS ONE* **7**, e38197, https://doi.org/10.1371/journal.pone.0038197

52 Weng, Y.S., Tseng, H.Y., Chen, Y.A., Shen, P.C., Al Haq, A.T., Chen, L.M. et al. (2019) MCT-1/miR-34a/IL-6/IL-6R signaling axis promotes EMT progression, cancer stemness and M2 macrophage polarization in triple-negative breast cancer. *Mol. Cancer* **18**, 42, https://doi.org/10.1186/s12943-019-0988-0

53 Raitoharju, E., Lyytikainen, L.P., Levula, M., Oksala, N., Mennander, A., Tarkka, M. et al. (2011) miR-21, miR-210, miR-34a, and miR-146a/b are up-regulated in human atherosclerotic plaques in the Tampere Vascular Study. *Atherosclerosis* **219**, 211–217, https://doi.org/10.1016/j.atherosclerosis.2011.07.020

54 Castro, R.E., Ferreira, D.M., Afonso, M.B., Borralho, P.M., Machado, M.V., Cortez-Pinto, H. et al. (2013) miR-34a/SIRT1/p53 is suppressed by ursodeoxycholic acid in t he rat liver and activated by disease severity in human non-alcoholic fatty liver disease. *J. Hepatol.* **58**, 119–125, https://doi.org/10.1016/j.jhep.2012.08.008

Table S1. The echocardiographic analysis of cardiac parameters in mice after treated with aldosterone for 42 days.

	WT-PBS	KO-PBS	WT-Aldo	KO-Aldo
Heart rate (Beats/min)	464 ± 24*	471 ± 15*	495 ± 37	480 ± 19*
EF%	70.32 ± 2.45***	75.98 ± 4.16***	46.11 ± 11.38	60.31 ± 12.12**
FS%	46.12 ± 2.93***	47.32 ± 5.32**	30.14 ± 7.03	40.12 ± 3.02**
LVAW;d (mm)	0.81 ± 0.27***	0.79 ± 0.15***	1.47 ± 0.36	1.05 ± 0.23**
LVAW;s (mm)	1.19 ± 0.26***	1.01 ± 0.19***	1.87 ± 0.43	1.42 ± 0.15**
LVID;d (mm)	3.46 ± 0.19**	3.13 ± 0.24**	4.66 ± 0.53	4.10 ± 0.32**
LVID;s (mm)	2.01 ± 0.19*	2.31 ± 0.17*	2.99 ± 0.53	2.43 ± 0.32*
LVPW;d (mm)	0.71 ± 0.18***	0.73 ± 0.12***	1.45 ± 0.43	0.92 ± 0.32*
LVPW;s (mm)	1.12 ± 0.17***	1.21 ± 0.21***	1.76 ± 0.32	1.42 ± 0.32*
LV Mass (mg)	117.43 ± 5.34***	125.26 ± 5.43***	198.53 ± 43.64	150.17 ± 16.74**

Data are means ± SEM. EF: ejection fraction; FS: fraction shorten; LVAW: left ventricular anterior wall, LVID: left ventricular internal dimension, LVPW: left ventricle posterior wall thickness, LV mass: left ventricle mass. *$p < 0.05$, **$p < 0.01$, ***$p < 0.001$, as compared with WT-Aldo group.